NRL REPORT 4075

CHARGING PROCEDURES FOR SUBMARINE STORAGE BATTERIES

E. E. Nelson, Isabelle M. Paige
and J. J. Lander

Electrochemistry Branch
Chemistry Division

November 7, 1952

NAVAL RESEARCH LABORATORY

WASHINGTON, D.C.

ABSTRACT

Charging data was collected for OWTX and VLA submarine cells which allow construction of TVG curves and which show rates of active material conversion. Heating data may be calculated on a theoretical basis. Combination of such data enables the construction of charging curves for any kind of charge so that best charging procedures can be established; typical curves constructed from the data are given. It is shown that maximum allowable gassing rates limit charging rates and times, where efficient cooling is available; in the absence of such cooling, temperature changes are the limiting factors. It is shown that only a small amount of experimental data is necessary to enable best charging procedures to be determined, and the process is reviewed for an MAQ cell. The effects of cell age and negative plate construction on charging procedures are discussed briefly.

PROBLEM STATUS

This is an interim report on the problem; work is continuing.

AUTHORIZATION

NRL Problem CO5-17
RDB Project NS 677-095

Manuscript submitted October 2, 1952

CONTENTS

CHARGING PROCEDURES FOR SUBMARINE STORAGE BATTERIES

INTRODUCTION

At the present time, charging procedures for submarine storage batteries are governed by three factors: first, the current capacity of the power source; second, a temperature-voltage-gassing relationship (the TVG curve) for the lead-acid cells which make up the battery; and third, the finishing rate. Charging procedures recommended for service use are essentially the same, but they may differ somewhat during the first stage of charge because of the first of the above factors and during the second stage because of the degree of voltage control available. They all become the same at the finishing rate during the overcharge period. This report will be concerned primarily with the first two stages of charge, the third or overcharge period being considered fixed either by the manufacturer's recommendation, or by the maximum safe gassing current for the submarine ventilation system.

To forestall the danger of fire and explosion in the submarine or injury to the plates of the cells themselves it is necessary to prevent the batteries from gassing too strongly during charge. For this reason, charging rates and voltages are referred to the TVG curve which has been established to automatically prevent danger. The curve in present use was established on the basis of previous work (1, 2, 3), which was done either on cells of designs which are now outmoded or on small portable cells. Consequently, it was considered desirable to re-establish the TVG curve for cells of modern design (4). As a result, data has been obtained by which new TVG curves could be established for cells of the later OWTX-49 and VLA-47 designs; but because of recent rapidly changing battery power requirements and negative plate characteristics cells of even newer design are being used, and the TVG curves which could be established from this work may be rendered outmoded also. Nevertheless, it is believed that the whole subject is in need of thorough review and that the general principles which have evolved from the new work will be applicable to any type cell and will enable future charging procedures to be established quite easily.

THEORETICAL AND PRACTICAL CONSIDERATIONS

The charging process in the lead-acid cell is an electrochemical reaction which consists in the conversion of $PbSO_4$ to Pb and PbO_2. It is accompanied by a secondary reaction whereby water is electrolyzed to hydrogen and oxygen gas. Many electrochemical processes require comparatively large values of overvoltage or polarization, i.e., values of energy which are larger than those theoretically necessary to bring about the reactions concerned—if they are to take place at appreciable rates. The extra energy generally shows up in the system, for the most part, as heat. Cases in point are the reactions mentioned above. The overvoltage accompanying the conversion of $PbSO_4$ is of practical importance because of its effect on the rate of the process and because of the extra energy requirement. In relation to submarine battery installations, it is more important because of its heating effect on the cells, which can affect markedly the rate of the gassing reaction. This, in turn, can

produce explosive gas concentrations and further heating, and it must therefore be controlled. The necessity for control results in prolonged charge times which contribute to the operational inefficiency of the submarine. Consequently, both the reactions and their interrelations will be considered in detail to show the limits imposed on charging rates and also to show how charging procedures may be developed for cells of new design.

When hydrogen and oxygen are generated electrochemically, the flow of current is produced only by relatively large values of polarization. This phenomenon is illustrated in Figure 1. The voltage at D in the graph used to be called the decomposition potential, and it was thought to be the voltage at which gassing began to take place, hence the concept of minimum gassing potential. Actually, it probably has no theoretical significance and does not represent a point of minimum gassing, but rather the curve takes its shape from the logarithmic nature of the relationship ($V \propto \log I$). Practically, it does have significance because it is the voltage at which appreciable currents begin to flow, and thereafter the current rises rapidly with small increases in voltage. Appreciable currents mean appreciable rates of hydrogen gassing and possible danger to the submarine, so that the recognition of a minimum gassing potential in setting up a TVG curve for control of submarine battery charging procedures was by no means without foundation.

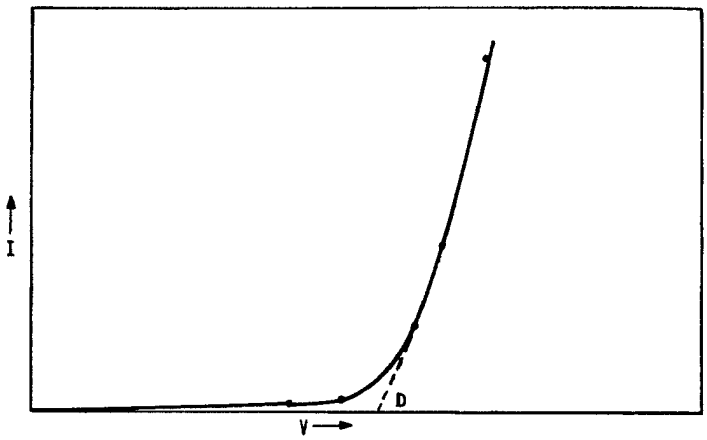

Figure 1 - Gassing current vs. voltage

It is apparent that the TVG curve is another way of plotting gas overvoltage data wherein temperature is used as the independent variable rather than current, and current (or gassing rate) becomes the parameter in place of temperature.* Consequently, gas overvoltage theory, and in particular hydrogen overvoltage theory, will be applicable to the lead-acid cell. At present, such theory seems to be in a state of considerable flux; accordingly, no attempt will be made to stress it here. However, several empirical generalizations are evident from the existing work, and they should make useful guides to thinking on the subject.

First, the higher the temperature the lower the overvoltage will be at a given current, or conversely, at the same overvoltage, higher temperatures result in higher gassing rates. This is obvious from the TVG curve itself and is, in fact, the reason for its existence. Second, at constant current and temperature, overvoltage depends on the area of metal surface exposed to the electrolyte. For example, in a 15 ampere-hour (AH) cell, a current of 2 amperes may produce a cell voltage of 2.6 on overcharge, but it may take 300-400 amperes to produce the same voltage in a submarine cell. Third, increasing acidity (in the higher ranges used in battery acid) results in lower overvoltage and so in higher gassing. This

*Among many others, Rideal, J.A.C.S., 42:94-105 and 749-756 (1920) will serve as an example

effect is not important in acid gravities of about 1.275 and below. Last, hydrogen overvoltage is markedly affected by the composition of the metal at which it occurs. For example, at the same current density it is considerably lower at a lead surface poisoned by antimony than it is at a pure lead surface. This effect is of very great practical importance in submarine battery installations because it results in marked decreases in charging efficiency, and it is generally responsible for poor performance of the negative plate in the lead-acid cell. Recent trends toward pure lead grids or lead-plated antimonial grids have in a large measure overcome this; but because antimony is still produced on the negative plate after corrosion out of the positive grid, its poisoning effect must be considered. Three of these four factors will be of fundamental importance in influencing charging procedures.

EXPERIMENTAL WORK

Submarine cells of three types were used; an OWTX-49, a VLA-47, and an MAQ-71. The first two were discharged to about 10,000 ampere hours at 500 amperes and then recharged at various rates and starting temperatures. Cell temperatures, total gassing rate, % hydrogen, current, and cell voltage were recorded automatically throughout the course of the charge. Single plate potentials were also measured, but they are not used in data correlation and will not be given. The first 25-30 cycles during the life of the OWTX and the VLA were spent in developing the experimental technique; after this, data was obtained for about 30 charges on the former cell and for about 50 charges on the latter. Somewhat over half the charges on the VLA were run at constant potentials of 2.4, 2.5, and 2.6 volts. Many of these included charges run after discharges of about 5500 AH rather than after discharges of 10,000 AH.

Gassing rates are reported corrected to 80^0 F and 760 mm pressure, so that 3.06 liters of hydrogen are equivalent to 400 amperes of current.

Six constant-voltage charges were run on the MAQ cell, which had been discharged to different amounts up to 7,000 AH and the same kind of data was collected.

The specific gravity of the electrolyte in all cells was 1.250 in the fully charged condition.

TYPICAL DATA COLLECTED

For the sake of brevity, it is not considered necessary to present all the charging graphs which were obtained. Instead, typical charge-data plots are shown in Figures 2 and 3. Figure 2 represents the data taken for a constant-current charge at 500 amperes, while Figure 3 shows the data obtained during a constant potential charge at 2.5 volts. As indicated on the graphs, the VLA Cell was used in each instance. With reference to Figure 3, the previous discharge amounted to 10,875 AH; and it can be calculated from the data that this amount had been returned to the cell in 4.45 hours. Because some of this current had gone to produce gas, a running correction was necessary to find the state of charge at any time after gassing started. If it is assumed that full charge was put in the negative plate when the theoretical rate of hydrogen gassing was reached then, by comparing the current with the gassing rate, the time at which full charge was accomplished can be obtained by inspection of the data. Working back from this point, the state of discharge at any time can be calculated. State of discharge is defined as the number of ampere hours of charge remaining to convert completely the $PbSO_4$, exclusive of gassing current. This is labeled on the time axis of the graphs in thousands of ampere hours out (AHO). It is based on the negative plate data because subsequent treatments of the data are concerned with the negative plate which is the producer of hydrogen gas.

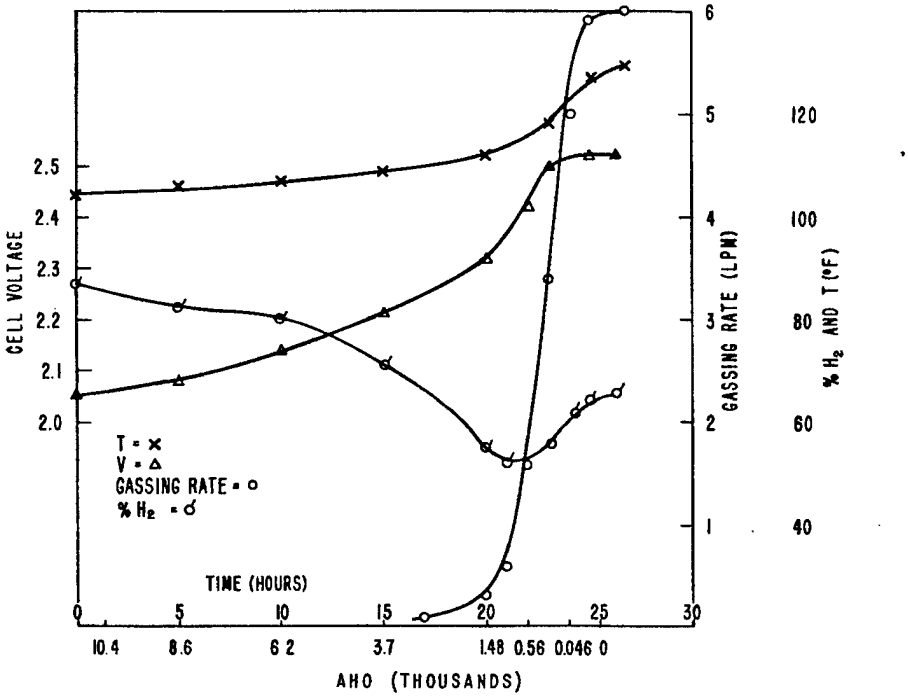

Figure 2 - Constant-current charge (500 amperes), VLA-49

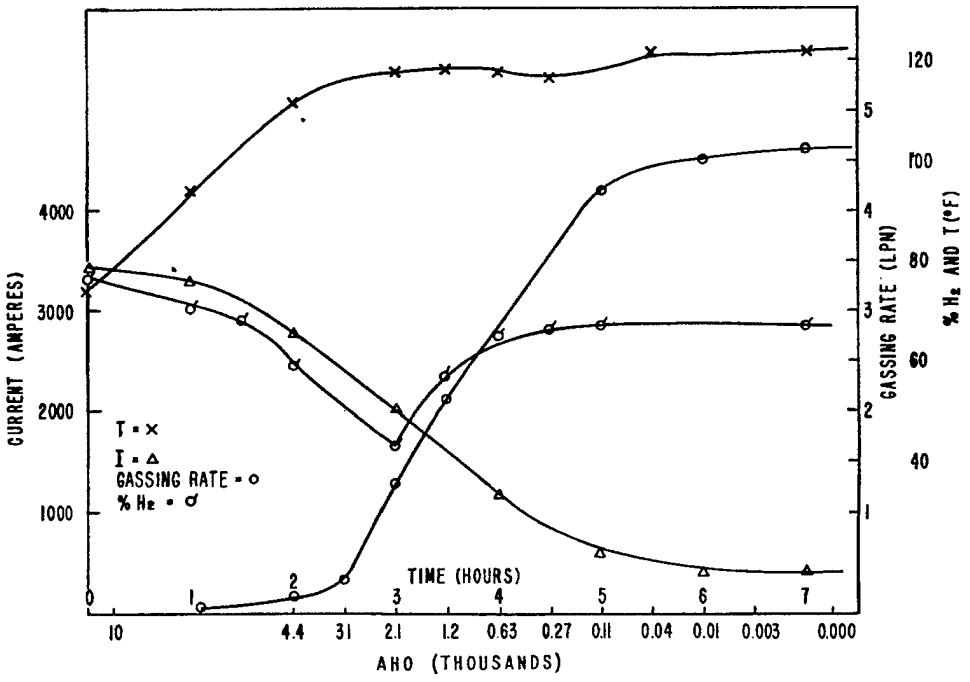

Figure 3 - Constant-voltage charge (2.5 volts), VLA-49

The same calculations could be made for the positive plate. The % hydrogen data shows that the positive plate begins to gas first, which means that both plates do not accept charge at the same rate at the same time. (Charge acceptance is defined as the rate of the reaction $PbSO_4 \longrightarrow Pb$ (or PbO_2) under any particular set of conditions; it always has the units of current in this report.) Actually the difference is not enough to be of significance, so that practically there is no difference between the charge acceptance at both plates. It can also be shown that the positive plate never gases at a rate greater than the finishing rate; so no danger to the positive plate will be expected to result from basing all conclusions on negative-plate performance.

At any rate, in making the comparison of current and gassing rates, reference to Figure 3 will show that full charge was put in at 7.5 hours and 99% of the charge was put in in 5 hours. This serves to illustrate the difficulty with which the last remaining $PbSO_4$ is converted. Similar remarks could be made concerning Figure 2.

GASSING RATES

With the AHO plotted on the graphs, the gassing rate can be determined at any desired state of discharge at the corresponding voltage and temperature. The series of charges was planned so that the latter two conditions would be different for different charges, so that a range of gassing-rate values would be obtained at any number of AHO. Some duplication occurred, but enough charges were run so that the temperature and voltage ranges are reasonably covered. The hydrogen gassing rate in amperes is plotted for 0, 500, 1,000, and 2,000 AHO as a function of voltage for the VLA and the OWTX in Figures 4 and 5 respectively. Temperatures are marked at each point. To avoid confusion, duplicates are not marked, and points are averaged when their temperature and voltages are within $5^{\circ}F$ and 0.03 volts respectively. As can be seen by reference to the figures, the experimental variation is well outside these limits; so nothing was lost in the process. Theoretically, a more reasonable plot would be amperes vs. the negative single-plate potential; but the data is more useful when the H_2 rate is plotted against cell voltage because single-plate potentials are not measured in service. Moreover, such plots were made, but they failed to make the data more regular; so that although variations in positive plate voltage are included they are small and unimportant compared to those for the negative-plate data.

From the data for the VLA cell, it can be seen that gassing rates fall off rapidly as the amount of charge remaining to be put in gets larger. This is also true of the OWTX cell, although it is a worse gasser and the effect is not pronounced until 1,000 AHO is reached. The results are quite scattered; nevertheless, as expected, there is a definite tendency for higher gassing rates at higher temperatures and voltages.

LOCATING THE TVG CURVE

Because gassing rates are highest at full charge, those rates for full charge may be used to locate the TVG curves. In Figure 6 the full-charge data is plotted in the usual fashion for a TVG curve for the VLA and the OWTX Cells. The numbers at each point show the hydrogen gassing rate in amperes. All the data are not plotted; those corresponding to gassing rates less than 250 amperes are left out as inconsequential. In each plot the data have been arbitrarily divided into two groups of cycles, one corresponding to charges made early in life and the other to late-life charges. In Figure 12 straight lines have been drawn through the data marked 315 and 400 amperes. These lines represent the minimum estimated voltage-temperature curves for the above values of gassing current for the early cycles. The points for the later group of cycles lie generally to the left and below these lines, where comparison is possible. This means that the TVG curve has dropped as the cell aged. Thus, charging voltages and temperatures which are safe early in life are no longer safe as life increases, and the TVG curves should be redetermined as cells get older in service. The aging effect is well-defined for the OWTX cell, as may be observed from Figure 13, where the dotted line represents the TVG curve for the cell later in life.

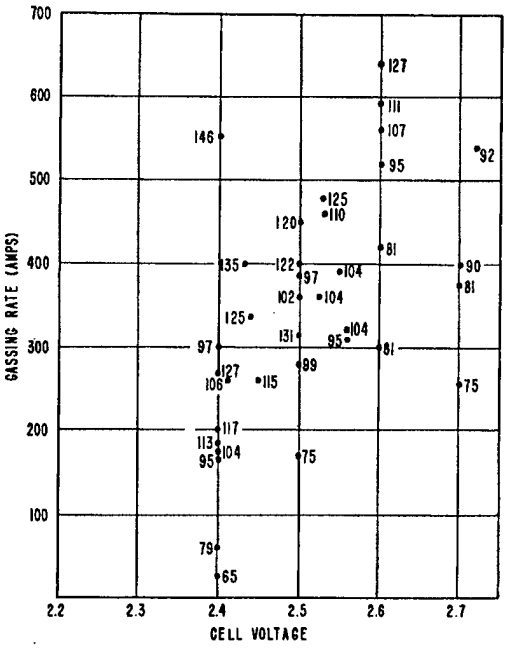

(a) Zero AHO

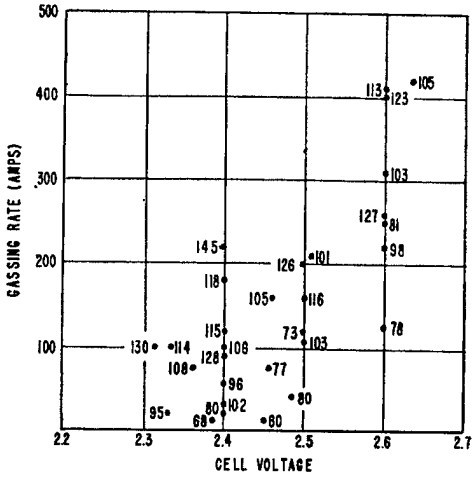

(b) 500 AHO

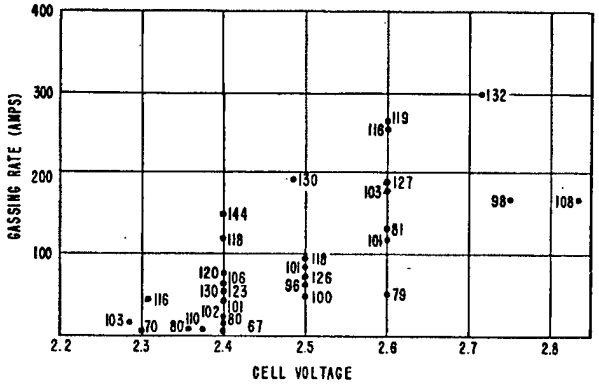

(c) 1000 AHO

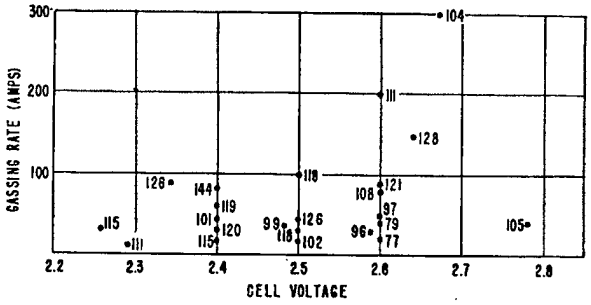

(d) 2000 AHO

Figure 4 - H_2 evolution vs. cell voltage, VLA cell; numbers at points are cell temperatures

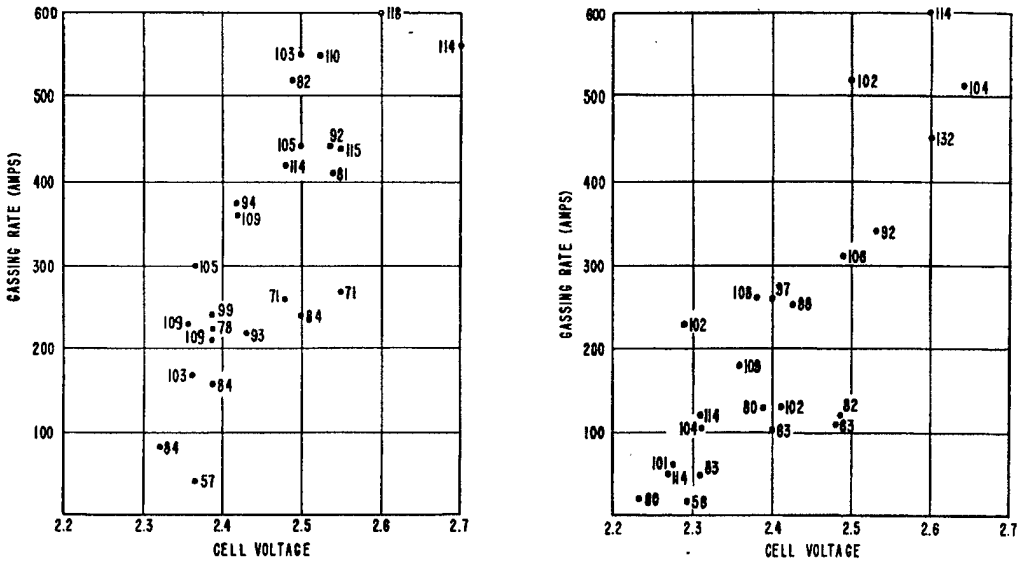

(a) Zero AHO

(b) 500 AHO

(c) 1000 AHO

(d) 2000 AHO

Figure 5 - H_2 evolution vs. cell voltage, OWTX cell; numbers at points are cell temperatures

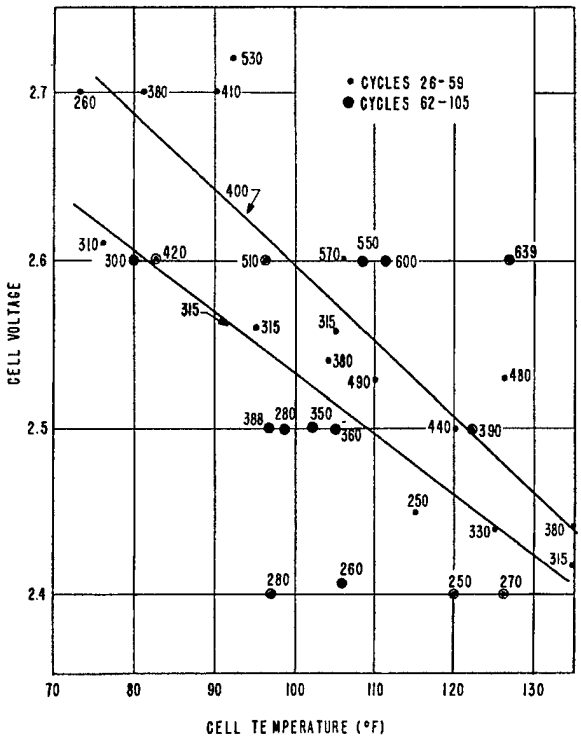

(a) VLA cell

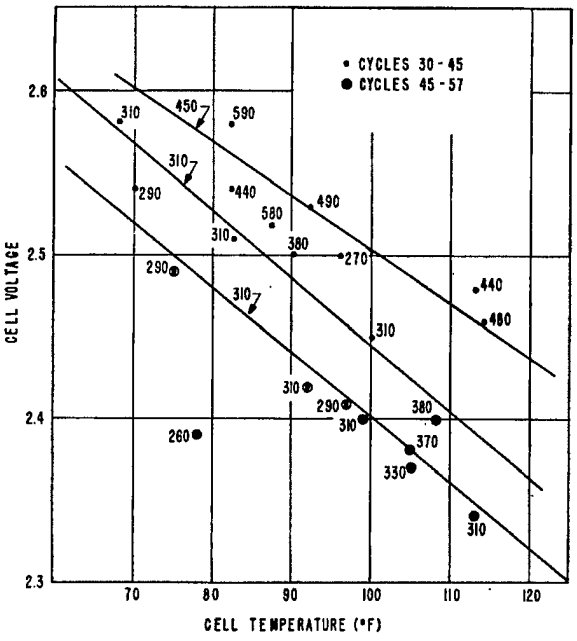

(b) OWTX cell

Figure 6 - Full-charge gassing data; numbers at points are H_2 gassing rates in amperes

The aging effect on gassing is generally considered to be due to the gradual accumulation of antimony on the negative plate, resulting in lower hydrogen overvoltage and, consequently, higher gassing rates at comparable temperatures and voltages. This may be particularly well-marked in the OWTX for several reasons: first, the initial TVG curve for the OWTX is lower than that for the VLA, which may possibly result in lower efficiency in gassing the antimony off the negative as stibine; second, the OWTX received more low-rate low-voltage charges than the VLA, and no attempt was made to keep the negative healthy in the accepted fashion; and third, the OWTX has a considerably larger positive grid area to supply antimony to the solution. The treatment received by the OWTX corresponds more or less to that which is currently run as an "Abuse Test" at the Material Laboratory. At the end of the test period the voltage at the finishing rate could not be brought back by ordinary charging procedures.

The hydrogen gassing rate has been used here to establish the TVG curve rather than total gassing because it allows a higher TVG curve, which will in turn be expected to allow faster charging, with a maintainance of safe gas concentration. Thus, if the individual cell were being ventilated at the rate of 4 CFM (equivalent to 113 LPM) at the finishing rate, then the hydrogen concentration would be maintained at 3% in the whole system if the cell were gassing hydrogen at 3.4 LPM. This rate of gassing is equivalent to 445 amperes. Thus, a double safety factor has been allowed because ventilation rates as high as 6 CFM are available in service. The higher finishing rates which would be allowed might help to keep the negative plate clean of antimony.

Figure 7 shows a comparison of various TVG curves which have been established. Curve 1 is that for the Tudor 20-POR-820 cell given by Reference 1. Curve 2 is that established (2) for a WLH-29 Ironclad cell, which has a finishing rate of 310 amperes. At 310 amperes a ventilation rate of 4 CFM would keep the hydrogen concentration at 2.1%.

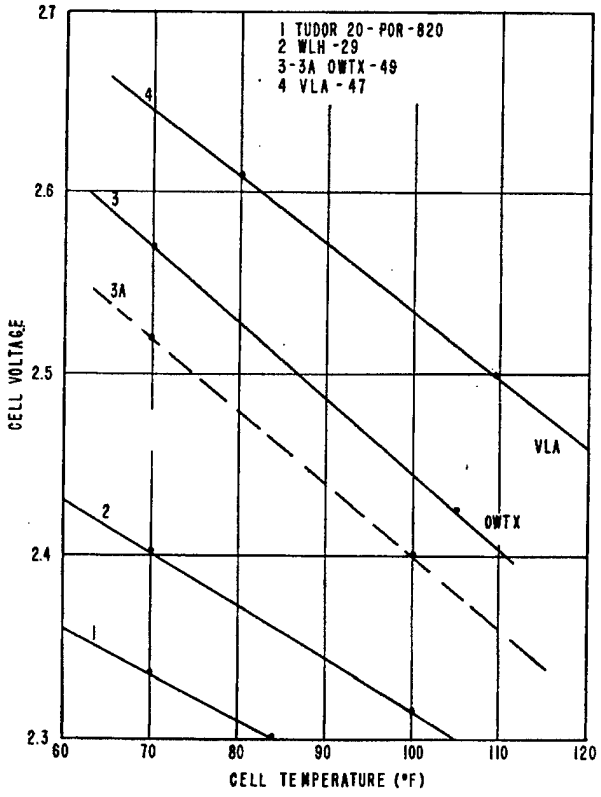

Figure 7 - Comparison of various TVG curves

It will be noticed that these curves have about the same slope. Theoretically, it is possible that TVG curves should have the same slopes regardless of cell design or state of charge because the TVG curve represents the temperature effect on hydrogen overvoltage which is found to be nearly constant for many metallic systems. It may also be said that the same reaction should have the same temperature effect. This is borne out to the extent of the precision available from the accumulated data in this report. Thus, the slopes of the curves of Figure 14 are 0.0025, 0.0029, 0.0042, and 0.0036. Additional values, obtained from the data of Reference 3, are 0.0038 and 0.0030 for Philco and Exide portable batteries respectively. Of course, these slopes all have a negative sign, and they average -0.0033 ± 0.0005.

It might be concluded that, ideally, TVG curves could be obtained from a single point; thus, the cell voltage and temperature corresponding to the maximum allowable gassing rate on the basis of cell ventilation could be obtained at the end of one charge. This point would be plotted on a rectilinear voltage-temperature graph and a line with the slope -0.0035 drawn through it. The process could be applied to a whole battery of cells in service.

Practically, it is not quite that simple because the slopes are actually found to vary with cell design, and perhaps with age; but worse, the variation of the data obtained in this work would certainly indicate caution in applying such a procedure. Nevertheless, if a log of such data were kept, a good idea of the safe maximum voltage-temperature combination would be at hand throughout the life of the battery because a minimum TVG curve for safe operation would be continuously established.

One other point may be made from the gassing data. It has been shown that gassing rates decrease rapidly as the amount of charge remaining to be put back in (AHO) increases. This means that the TVG curve is shifted upwards as AHO increases, so that the TVG curve established for a fully charged cell does not limit safe charging potentials and temperatures for the partially discharged cell. Therefore, in the interests of most rapid charging, initially higher voltages than those corresponding to the full-charge TVG curve might be used. The voltage would have to be cut back in such a way as to maintain hydrogen concentrations at a safe level until the voltage intersects the TVG curve, after which charging would proceed according to the curve. This procedure might be expected to result in high battery temperatures unless efficient cooling were available. Further treatment of the data will shed additional light on the matter of charging procedures.

CHARGE ACCEPTANCE AND MINIMUM TIME FOR COMPLETE CHARGE

From the data of Figures 2 and 3, the rate of conversion of $PbSO_4$ (i.e., the CA) may be calculated for the negative plate for the various states of discharge (AHO) by subtracting the gassing rate in amperes from the total current. This has been done for the data of Figures 2 and 3, and the results are plotted in Figure 8. Again the data is based on negative plate performance because the data shows that both plates accept charge at practically the same rate. The abscissa in this case is not time but AHO. Cell voltage and temperature are also plotted, so that their effect on charge acceptance could be obtained. From the data for all charges the CA vs. cell voltage at 10,000, 5,000, 2,000, 1,000, and 500 AHO have been plotted for the VLA cell in Figure 9 and for the OWTX cell in Figure 10. Temperature values are marked at each point. For the data, temperature effects seem to be small and of the order of experimental error or less. The effect of voltage is large and approximately linear. Figure 11 is a composite plot of the CA data.

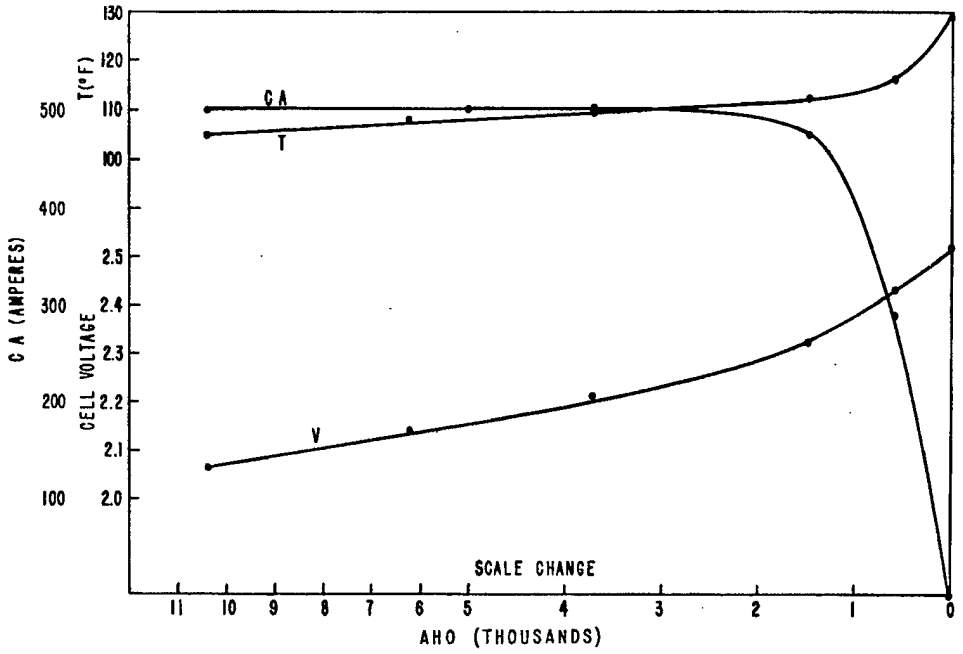

(a) Data calculated from Figure 2

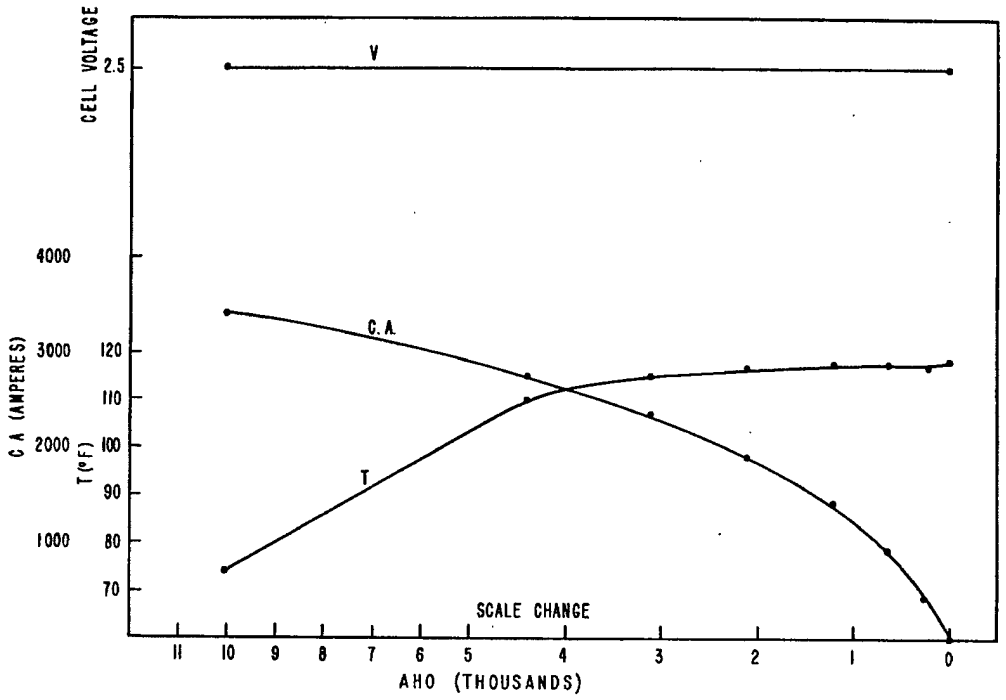

(b) Data calculated from Figure 3

Figure 8 - Charge acceptance vs. state of charge

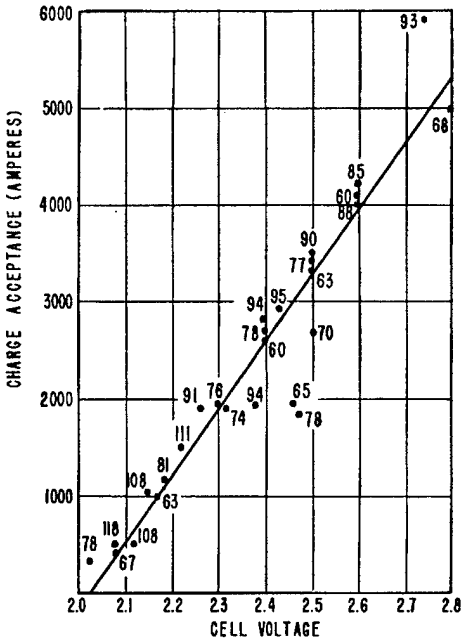

(a) 10,000 AHO

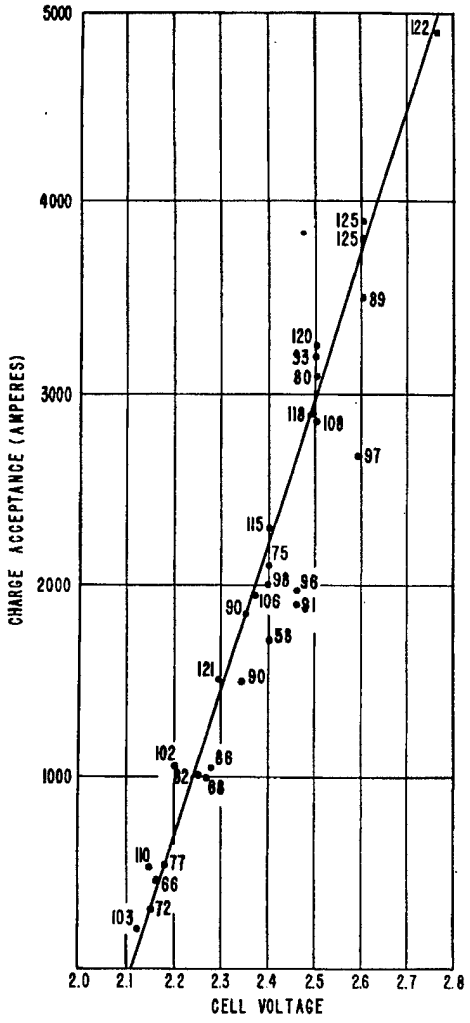

(b) 5,000 AHO

(c) 2,000 AHO

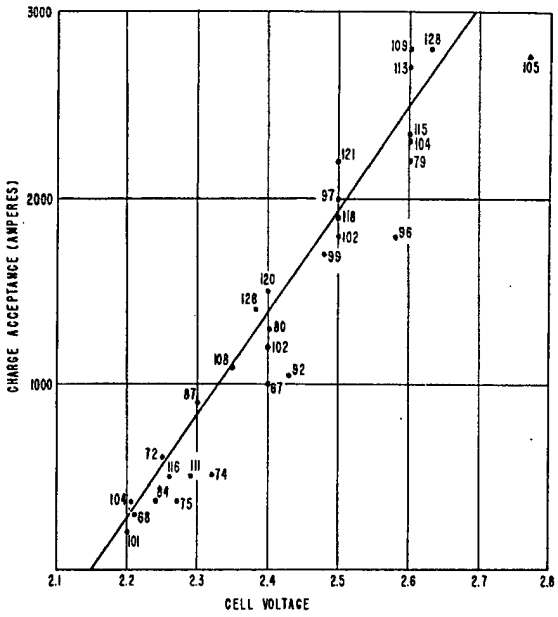

(d) 1,000 AHO

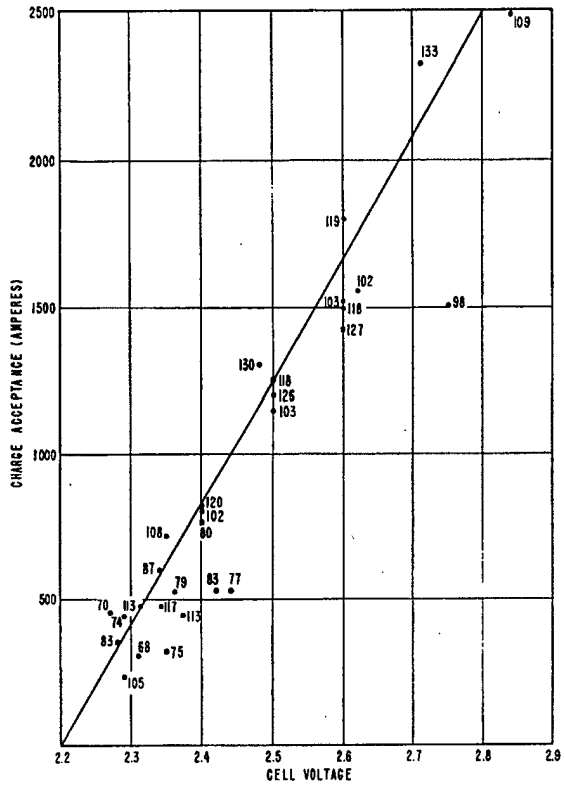

(e) 500 AHO

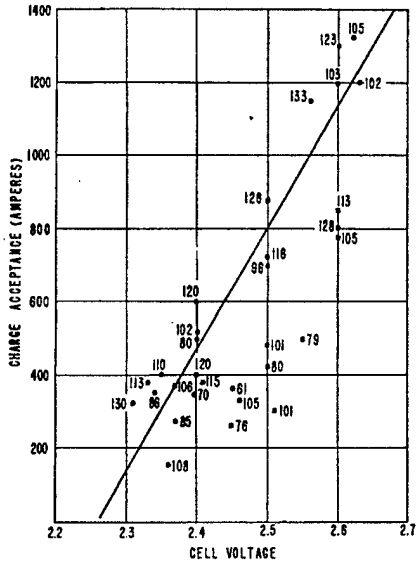

Figure 9 - Charge acceptance vs. cell voltage, VLA cell; numbers at points are cell temperatures

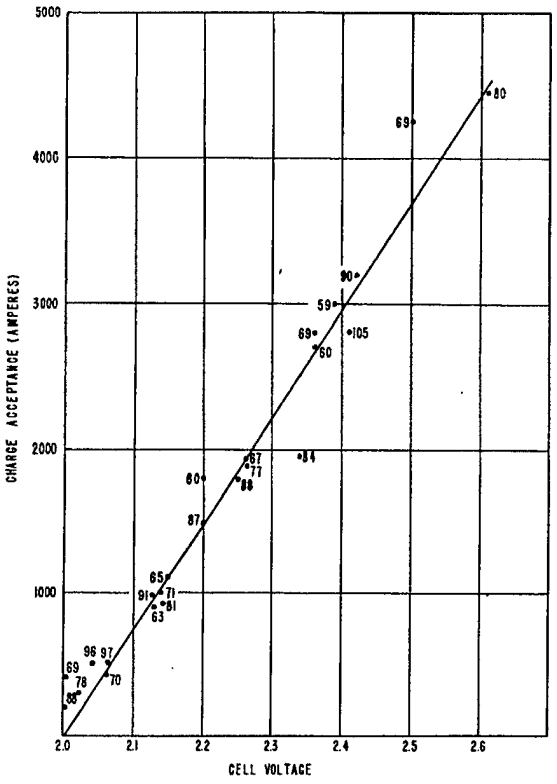

(a) 10,000 AHO

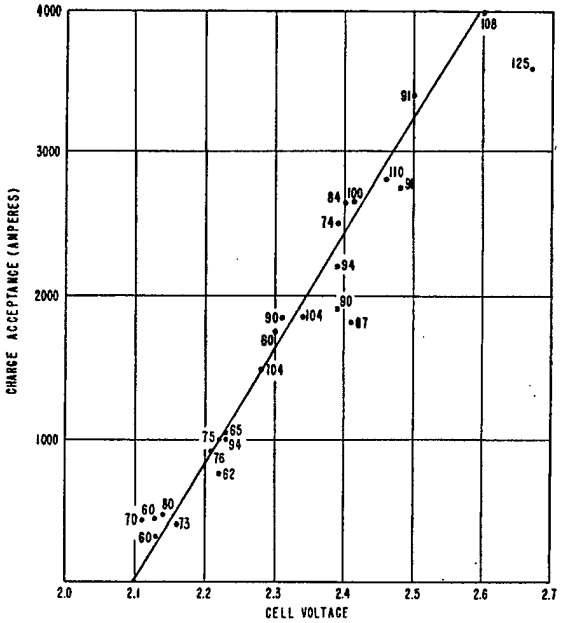

(b) 5,000 AHO

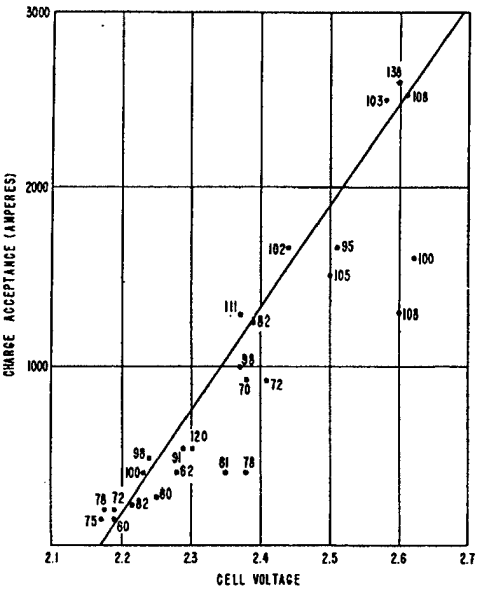

(c) 2,000 AHO

Figure 10 - Charge acceptance vs. cell voltage, OWTX cell; numbers at points are cell temperatures

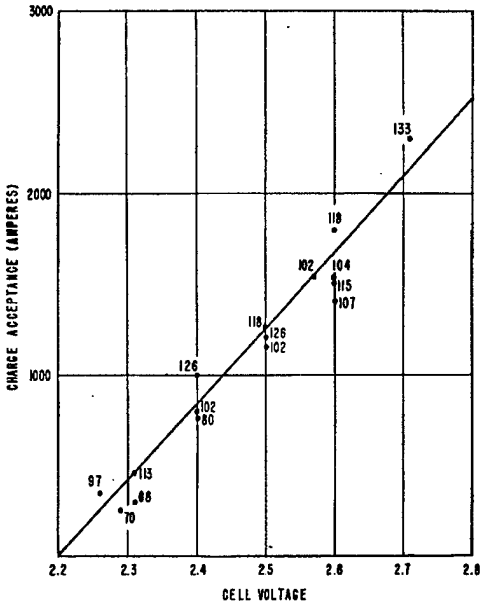

(d) 1,000 AHO

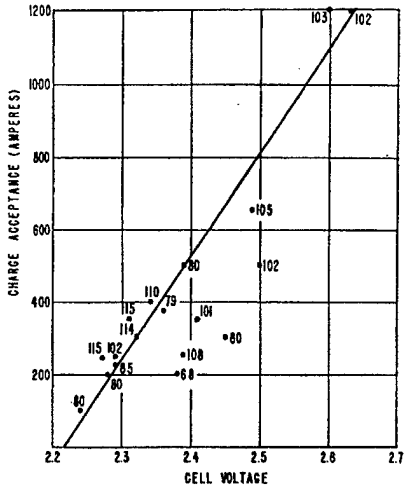

(e) 500 AHO

Figure 10 (Cont'd) - Charge acceptance vs. cell voltage, OWTX cell; numbers at points are cell temperatures

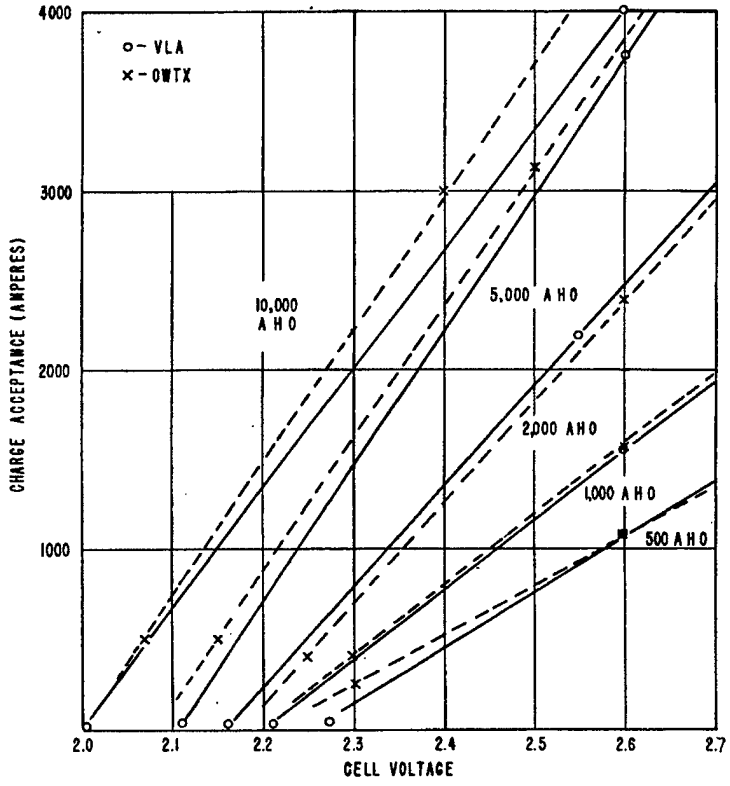

Figure 11 - Charge acceptance vs. cell voltage, VLA and OWTX cells

From this data, plots of CA vs. AHO at several potentials may be made as in Figure 12. These curves represent the rate at which $PbSO_4$ conversion would take place under a constant potential charge as the charge progresses. Moreover, since they are rates and are not very greatly influenced by temperatures within the ordinary operating ranges, it is a simple matter to calculate the minimum time for complete charge for any constant-potential charge. This was done by dividing each 1,000 AHO unit by its corresponding average current and adding up the increments obtained. When time for complete charge,* so obtained, is plotted against potential the solid curve shown in Figure 13 is obtained. It can be seen that it falls off much less rapidly as charging voltage increases, so that there would not be much use in pushing the charge voltage beyond 2.6 volts for these cells, because the time saved begins to become inconsiderable. However, there is a stronger limitation than this placed on maximum charging rates.

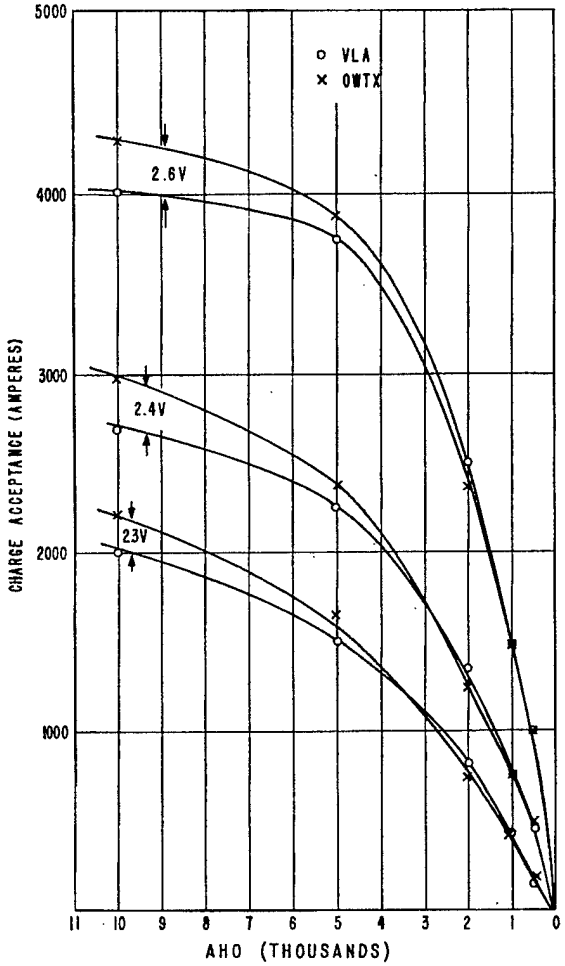

Figure 12 - Charge acceptance vs. state of charge at several voltages, VLA and OWTX cells

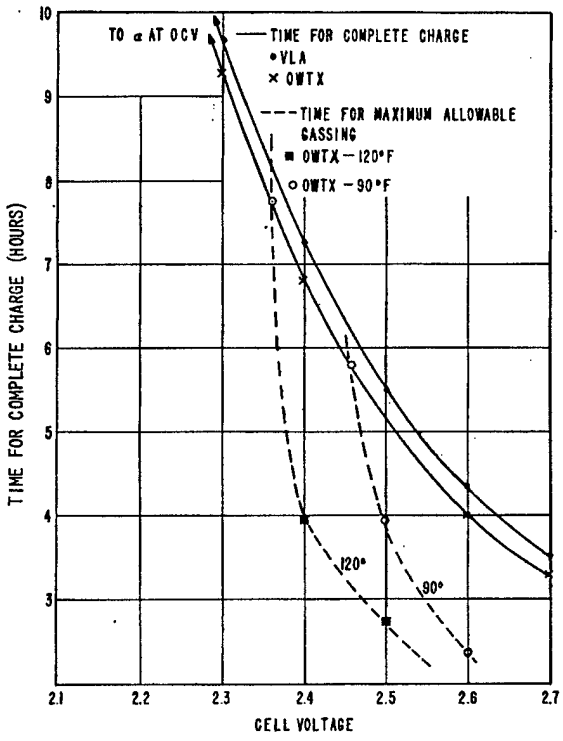

Figure 13 - Time for nearly complete charge at several constant voltages, VLA and OWTX cells

*These results actually represent more closely the time necessary to put in all but about 100-200 AH, because smaller increments must be used over the last 1,000 AH or so.

The solid curve of Figure 13 was obtained with no gassing restrictions. For purposes of calculation, it may be assumed that 310 amperes is the maximum allowable gassing rate. Then, from the gassing vs. state of charge curves, the value for AHO at which maximum gassing will be reached at any potential and temperature can be estimated. This has been done for the OWTX cell, and the results for 120^0 and 90^0 are plotted in Figure 13 as dotted curves. The points at which these curves cut the complete-charge curve show the voltage at which the maximum gassing level will just be reached as the cell comes to full charge at the temperature concerned. If the charge were run at the constant voltage and constant temperature concerned, then the time for the complete charge would also be given by the point of intersection. Evidently, the time for full charge is limited chiefly by the temperature, once a maximum safe gassing level is assigned.

Now suppose that an OWTX cell may be maintained at 90^0F because it is equipped with a very good cooling system. Then, if a constant-potential charge were put in at 2.48 volts, full charge would be reached in 5.8 hours, the minimum possible time for those conditions by Figure 13. But if it were desired to put the charge in faster, it could be started at some higher voltage, say 2.6, and allowed to continue at that voltage until gassing came up to the maximum safe rate; this would occur at 2.4 hours from Figure 13. Then the charge voltage could be cut back gradually, maintaining the gassing constant, or it could be cut back at once to 2.48 volts with no further control necessary. For the latter method of charge the time required would be 5.1 hours, and a time saving of 0.7 hours would have been obtained. These two types of charges are illustrated by the curves of Figure 14 which were constructed from the charge-acceptance and gassing data for the OWTX cell. At 120^0F, the charging time would be appreciably longer, where 7.7 hours would be necessary to complete the charge at a constant voltage of 2.36, although this could be speeded up somewhat if higher voltages were used initially.

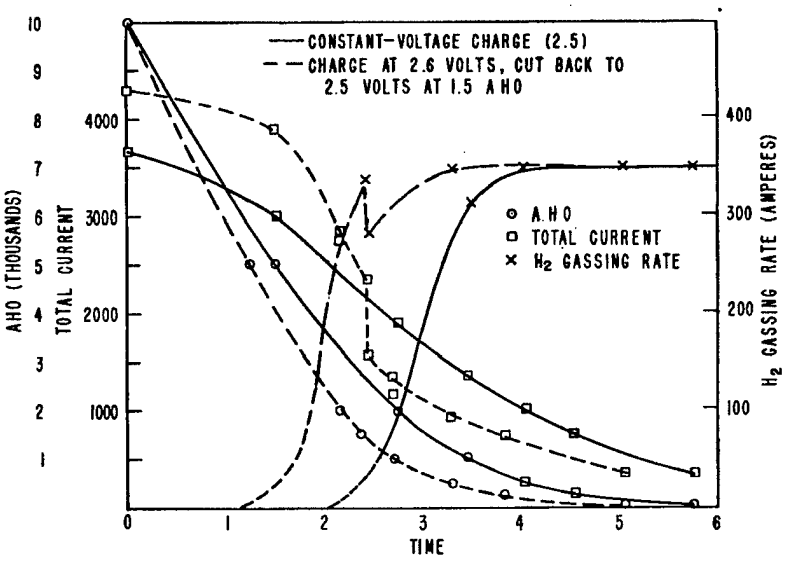

Figure 14 - Constructed charge data for charge at 90^0 F, OWTX cell

It may be pointed out that, where necessary in a series of cycles, very fast charges could be put in with the cell operating at some point under maximum capacity, if efficient cooling and electrolyte stirring were available. For these cells, at 90^0F, 80 to 85% of full charge can be returned in 2.5 hours with safety.

The points which make up the time-for-maximum-gassing curve of Figure 13 are fixed points on TVG curves for various states of charge; so they will be affected by those factors which affect the TVG curves. The temperature effect is obvious from the graph. Increasing age will lower this curve and result in longer charge times. It is supposed that the basic time-for-complete-charge curve will not be changed much by the factors of temperature and age. Perhaps it should be emphasized that there is nothing arbitrary about this data except the selection of a maximum gassing rate, since all other characteristics are fixed by the cell itself. In practice the maximum safe gassing rate will be fixed by such factors as ventilation rates and cell design.

HEATING EFFECTS

At this time, efficient cooling systems are not in general use in service; accordingly, high-voltage high-rate charges will be expected to result in high battery temperatures because the extra energy which causes heating is put in so rapidly that ordinary cooling factors simply do not have time to operate to any worthwhile extent. As explained previously, there are two sources of extra energy: one is the overvoltage of the conversion reaction; the other is the overvoltage of the gassing reaction.

If power units are used for a charge from 10,000 AHO, the extra amount necessary for $PbSO_4$ conversion is simply calculated as the difference between the minimum power required and that actually used during the charge. The minimum requirement is given by the product of the open-cell voltage and the number of AHO's (2.1 x 10,000 = 21,000 watt hours).* If a cell were to be charged at a constant voltage of 2.4, the total power input for the conversion reaction would be 2.4 x 10,000 = 24,000, and 3,000 watt hours over the minimum would have been supplied. This must show up in the cell as heat because it is doing no other appreciable work. The temperature rise can be found by converting the extra power to kcal and dividing by the heat capacity of the cell (5). For the OWTX this would be $3,000 \times 0.86 \div 80 = 32^{\circ}$ F.

Suppose that the 2.6-volt charge of Figure 14 had been run with no cooling, then $(2.6 - 2.1) \times 9,000 \times 0.86 \div 80 = 48^{\circ}$ F. The equation says that the cell temperature would have risen 48° in 2.2 hours (the time for 90-percent charge) due to the overvoltage of the conversion reaction alone. To maintain constant temperature the cooling system would have had to transfer 3,900 kcal out of the cell in 2.2 hours. Additional heating due to conversion of the last 10% of $PbSO_4$ would have raised the cell temperature 5.4° more.

When the cell starts to gas near the end of charge, still more heat is supplied by the overvoltage of the gassing reaction. The energy contributing to heating from this effect may be calculated from the equation $W = (V - 1.23 - 0.36) \times I$, where W is the energy in watts producing heat, V is the working voltage of the cell, 1.23 is the reversible potential for the reaction $H_2O \rightarrow H_2 + 1/2\ O_2$, 0.36 is the voltage equivalent of the entropy term, and I is the gassing current. If the gassing data for the constant-voltage charge at 2.5 of Figure 14 is used as an example, it can be calculated that from the time gassing started to the time charge was complete 866 watt hours had gone toward heat as the result of gassing. This amount would correspond to a 9.3° temperature rise for the OWTX cell.

*For the OWTX cell at 1.250 gravity, the reversible potential for a fully charged cell is about 2.10 volts. At 10,000 AHO, it is about 1.96, so that more exactly a running correction should be applied over the whole charge. This correction would decrease the minimum power requirement, and it could amount to as much as 700 watt hours. In addition, the entropy term for the reversible reaction is estimated to contribute about 600 watt hours to heating.

In Figure 15 is shown the extra energy which goes into heat as a function of voltage, assuming constant-voltage constant-temperature (90° F) charges from 10,000 AHO. It should be realized that when temperature is not controlled, charge times will be longer and gas volumes will be larger; accordingly, the gassing contribution will be larger. In addition, neither of the two corrections mentioned in the previous footnote were made.

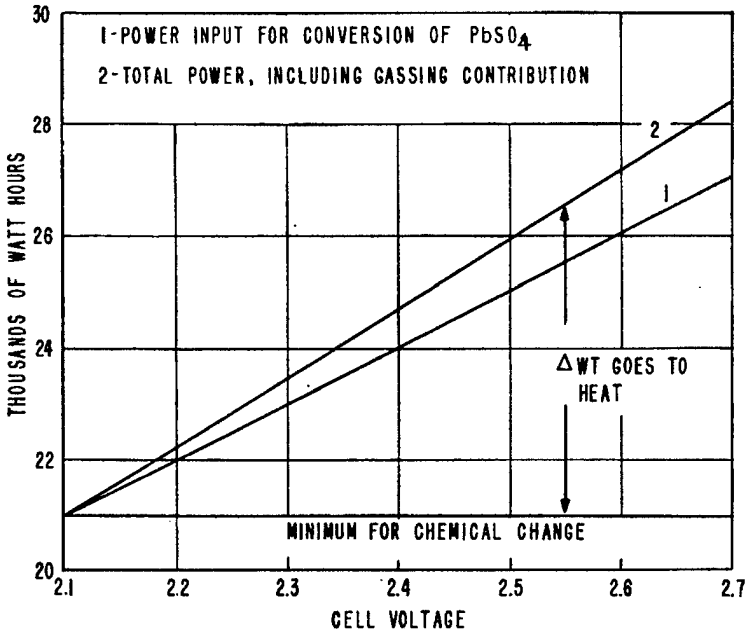

Figure 15 - Total power input and power contributing toward cell heating

To emphasize the very rapid heating which will occur on high-voltage high-rate charges Table 1 has been drawn up. It shows the change in temperature and the time period for the temperature rise which would take place in an uncooled OWTX for various constant-voltage charges. Again, these are minimum values because the various corrections have not been applied. For the VLA cell the temperature gains would be slightly smaller because it has a slightly higher heat capacity and does not gas so badly, and they would be spread over a slightly longer time. Table 1 shows that ordinary cooling effects, which might amount to 3-5° per hour (5), will hardly make a dent in the fast temperature rises associated with high-rate charges.

TABLE 1
Cell Heating for Constant-Voltage Charges (OWTX Cell)

Voltage	Heat Liberated (kcal)	Temp. Rise (°F)	Time (hours)
2.7	6360	80	3.3
2.6	5340	66	4.0
2.5	4200	52	5.2
2.4	3180	40	6.8
2.3	2140	27	9.3

TIME FOR COMPLETE CHARGE WITH NO COOLING

The heating data completes the-information necessary to enable preconstruction of charging-data curves for any sort of charge with no cooling. Some cell-cooling data is available (5) and could be used, if desired, to preconstruct charge curves for ordinarily available cooling. In this report only the extreme conditions of no cooling and efficient cooling will be considered to show how the data may be used.

To illustrate the effect that temperature increase has on gassing and total time of charge, the charging curves of Figure 16 have been estimated for the OWTX with no cooling. A comparison of these curves with those of Figure 14 shows how the time for complete charge is prolonged because of the temperature effect on gassing. Figure 16 also shows that where cooling is not available and full charge is necessary no time is saved by starting out at higher voltages and cutting back as gassing comes up. This is because the larger initial heating (along with the higher voltage) brings gassing up much quicker so that voltages must be cut back much earlier, and charging times are thereby actually prolonged. On this account, charging by the TVG curve could be, under some circumstances, a questionable procedure. However, 80% of charge can be put in in somewhat less time at the higher voltages, so that in service it might be possible to work cells rather hard at less than rated capacity if ordinary cooling is available.

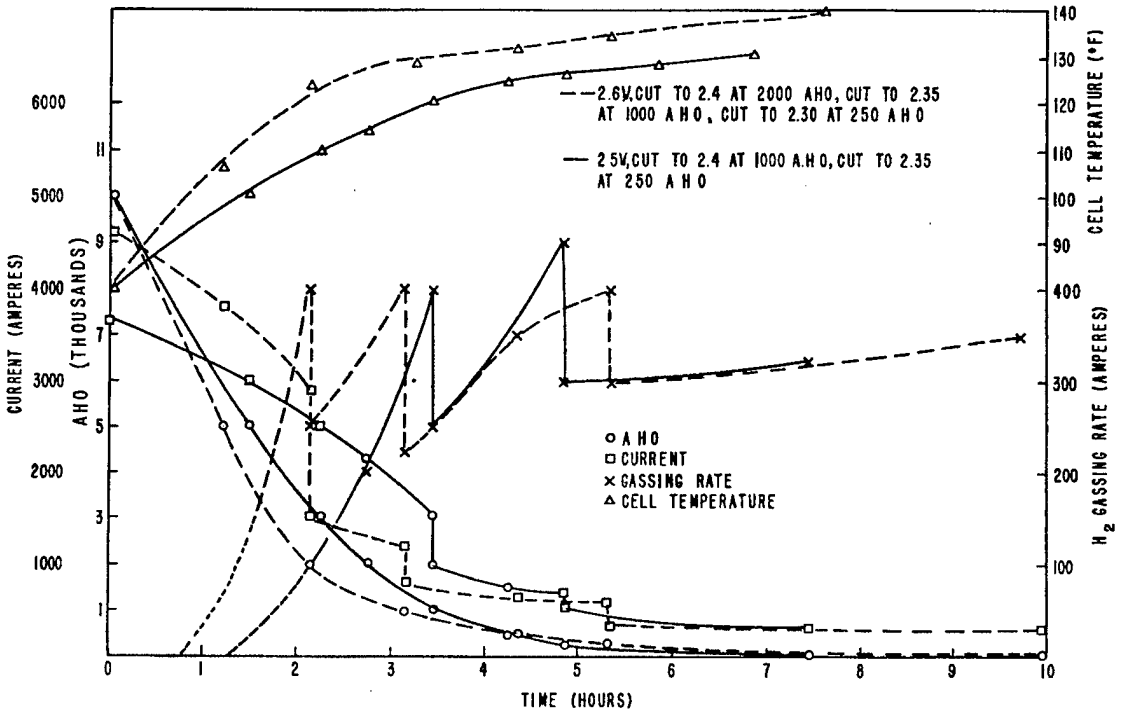

Figure 16 - Constructed charge data with no cooling, OWTX cell

INFORMATION NECESSARY TO ESTABLISH CHARGE PROCEDURES FOR NEW CELLS

So far, it has been shown that charging curves can be constructed for study on the basis of hydrogen-gassing data and cell-heating data. In this work, considerable time was spent in collecting a large amount of data on cells which were outmoded before the experimental work was finished. It is proposed to show that this is unnecessary and that with

comparatively little data, charging curves can be preconstructed for the latest cell designs for study to determine charge procedures. About six experiments would be necessary to obtain the same data collected in this work.

Approximate gassing curves could be drawn after six charges from maximum AHO– three at a constant potential of, say, 2.4 volts and finishing at temperatures over the range 80°-120°, and three at different voltages, say, 2.3, 2.4, and 2.5, but all finishing at nearly the same temperature. The gassing data for several AHO's would be plotted on semilog paper as cell voltage vs. the log of the gassing current. The three voltage points would establish the slope, and parallel lines could be drawn through the temperature points. The TVG curve would be established by plotting, in the usual fashion, the temperatures and voltages corresponding to the maximum gassing current, which, of course, would be based on the available ventilation, or perhaps the manufacturer's recommended finishing rate. The charge-acceptance data could be determined from the same set of experiments, although two additional runs to provide duplicates at the other two voltages would be desirable. The whole set of data might actually be determined from one charge arranged to go at such a constant voltage that a gassing rate somewhere near the maximum value would be reached at the end of charge. This would entail several assumptions: one, that the slope of the V vs. log I curve would be about 0.3-0.4; two, that the slope of the TVG curve would be about the average obtained previously; and three, that the CA vs. cell voltage curve is linear.

Cell heating under any desired charge can be calculated by means of the heating relationships provided and the experimentally determined gassing characteristics. The heat capacity could be summed up from the cell construction (5), or it could be estimated from the experiments themselves from the knowledge of the heating due to the conversion reaction and the observed temperature rise. (Cooling effects would have to be considered, but they are comparatively minor for high-rate charges.) All the necessary data would then be provided.

The process is reviewed below, where the six sets of charge data obtained for the MAQ cell are used for an example.

APPLICATION TO THE MAQ CELL

The experimental charges on a new MAQ cell were all run at constant voltage (2.4) for different states of discharge up to nearly complete discharge. A typical set of data is shown in Figure 17. The gassing data from these charges have been plotted in Figure 18 for the fully charged cell. Through these points are drawn lines with the slope 0.40, under the assumption that the hydrogen gassing rate follow approximately the relation established empirically for the other cells.* If it is assumed that 4CFM will be supplied to ventilate this cell in a submarine battery, than a maximum gassing current of 445 amperes could again be allowed; but because the previous data has been calculated on the basis of 310 amperes, the latter value will be used. Then, by picking from the curves the voltage values at which the temperature lines intersect the ordinate at 310 amperes, a typical TVG

*Ideally, the slope of log I vs. single-plate potentials probably should be near 0.11 for H_2 and O_2 gassing curves, and these should increase slightly with temperature, so that the cell voltage vs. log I curve should have the slope 0.22, and this will increase with temperature. It has been observed that antimonial negative plates may exhibit curves with slopes of 0.19 or higher, so that slopes for the cell voltage might be expected to be 0.30 and higher. In fact, for the VLA and OWTX these slopes are estimated from the gassing data to be about 0.6. Increasing values of these slopes would make the absolute value of the TVG slopes larger. Variations of the magnitude encountered do not seem to be of much practical importance.

curve may be plotted, as in Figure 19. Curves are plotted for both the fully charged cell and for the cell at 2000 AHO. The manufacturer's curve is plotted for comparison. The full-charge TVG curve has the slope -0.0041 which is in fair agreement with the slopes for the other cells. Thus, this cell may be charged with safety at voltages more than 0.1 volt higher than those recommended; with efficient cooling, this will result in appreciable saving of charge time, as will be shown.

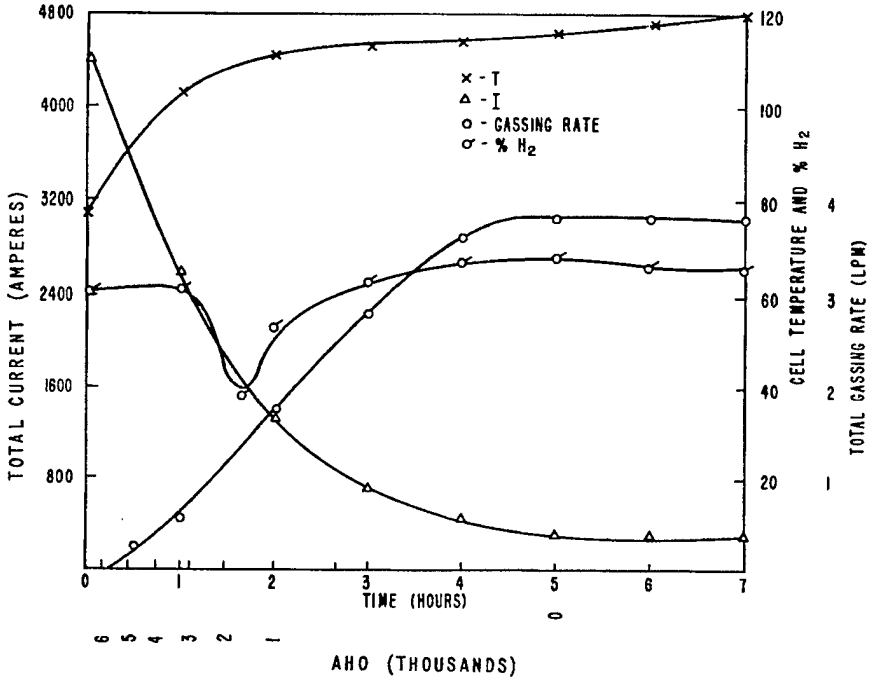

Figure 17 - A typical charge for the MAQ cell at 2.4 volts

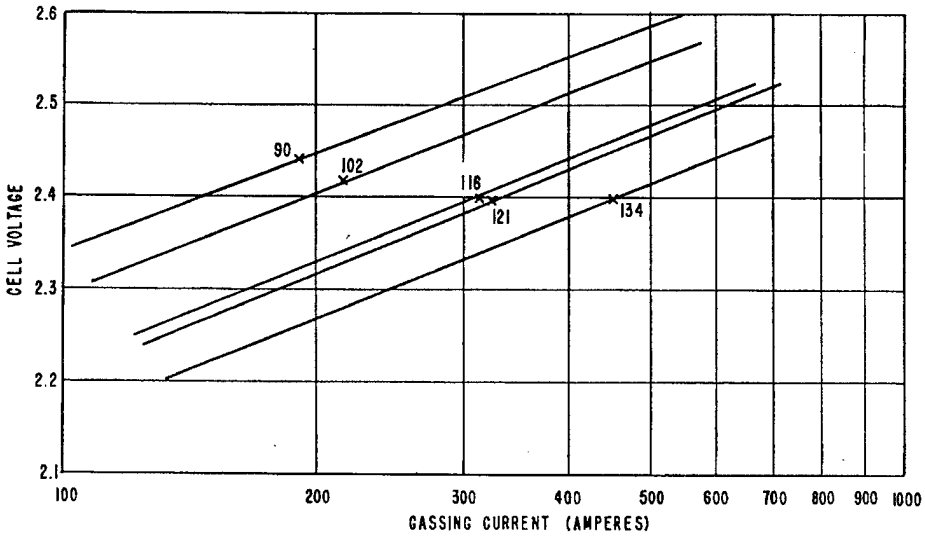

Figure 18 - Full-charge gassing, MAQ cell; numbers at points are cell temperatures

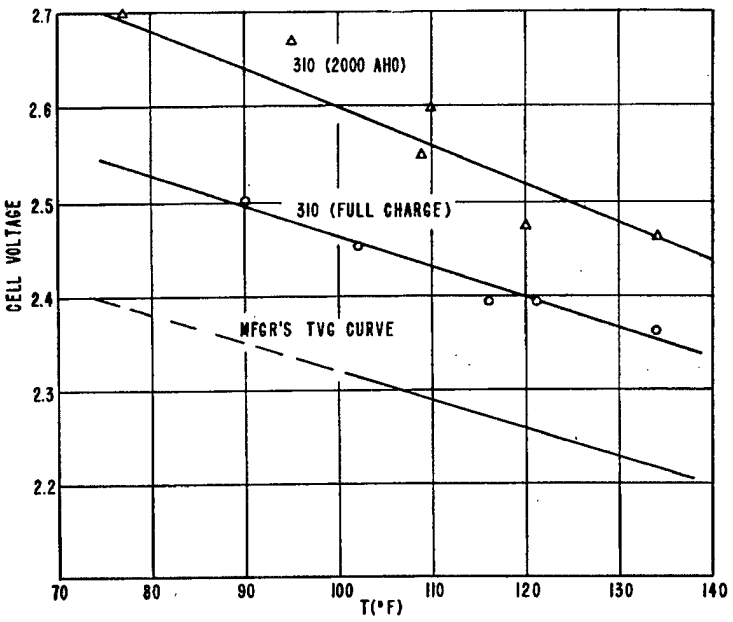

Figure 19 - TVG curve, MAQ cell

The charge acceptance data for various states of discharge is plotted in Figure 20. The temperature corresponding to each point is given, and it would seem that higher temperatures result in lower values of CA. However, the higher values of CA also correspond to previous smaller discharges, and it is believed that this is the significant factor.* At any rate, if it is true that smaller discharges result in higher values of CA, nothing but better performance than the calculated curves indicate could be obtained because they are all based on data for fully discharged cells. Then, if the CA is linear with voltage for this cell, as was found for the others, the curves of CA vs. voltage of Figure 20 may be drawn and those of CA vs. AHO of Figure 21 constructed from them. As before, the minimum time for complete charge at various constant voltages may be calculated, as well as the time to reach maximum gassing. These results are plotted in Figure 22. All the data necessary for preconstructing constant-temperature charge curves is now at hand. This has been done for a 7,000 AHO at 2.5 volts and 90° F and is illustrated in Figure 23. The results are compared in the same figure with a charge calculated using the recommended TVG curve and allowing the voltage to rise when the recommended finishing rate of 300 amperes is reached. Full charge under the latter procedure would take about 7.5 hours, whereas the former requires about 4.5 hours. 80% charge is put in in 4.1 and 2.3 hours, respectively.

For the cell with no cooling, it can be shown, by use of the experimental TVG curve, as in Figure 24, that a charge started at 80°F and 2.5 volts will be finished in about 5.5 hours. Temperature during this time would have risen to 135° F, if an estimated value of 54 kcal/°F for the heat capacity of this cell were used. This graph, in comparison with Figure 23, illustrates again how charge time is prolonged in the absence of efficient cooling as a result of the increase in cell temperature.

* This tendency is also indicated by comparing the CA data for the VLA cell for previous discharges of 10,000 and 6,000 AHO. The comparison was not included in the report because the effect was not large enough to obscure the data of Figure 11.

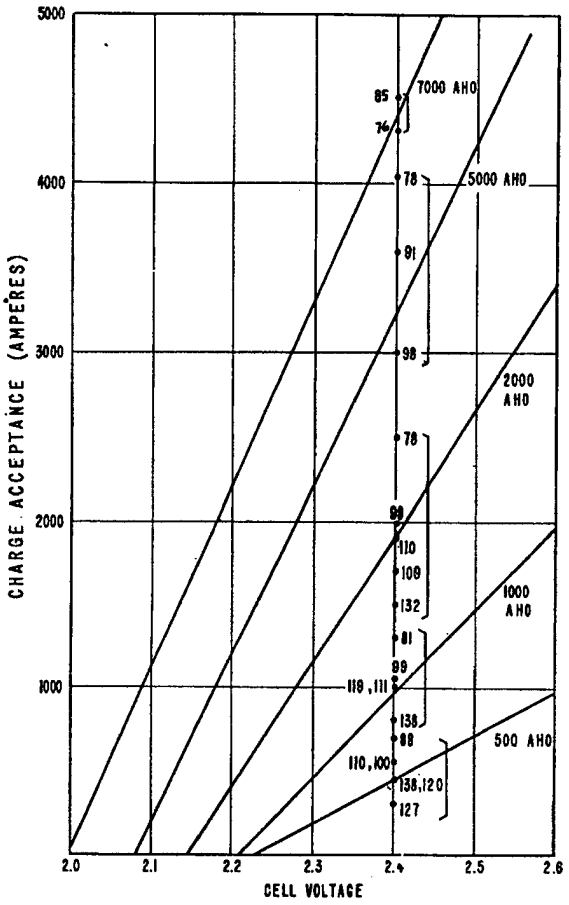

Figure 20 - CA vs. cell voltage, MAQ cell; numbers at points are cell temperatures

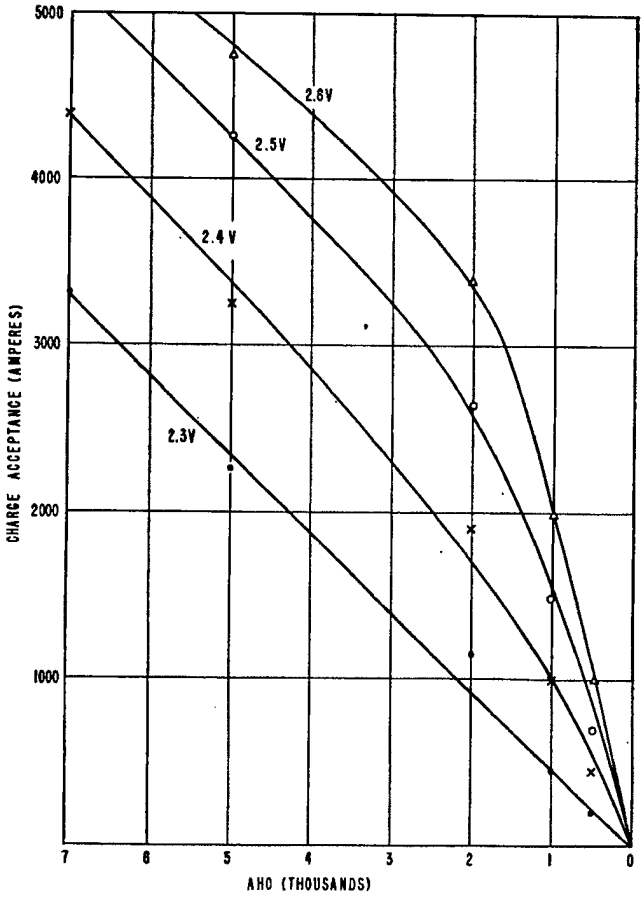

Figure 21 - CA vs. AHO, MAQ cell

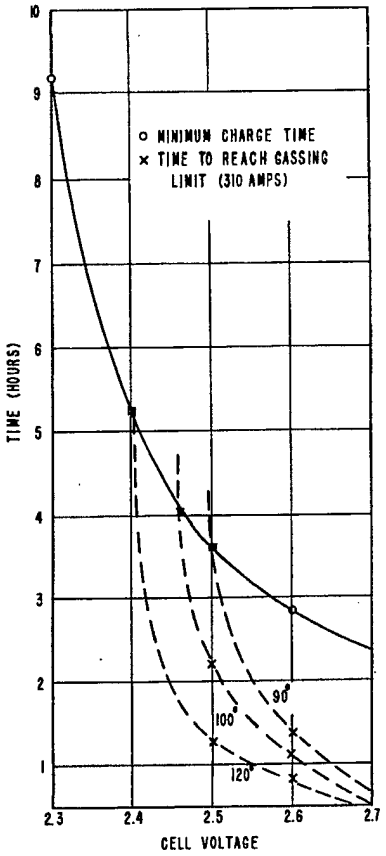

Figure 22 - Minimum charge time from 7,000 AHO, MAQ cell

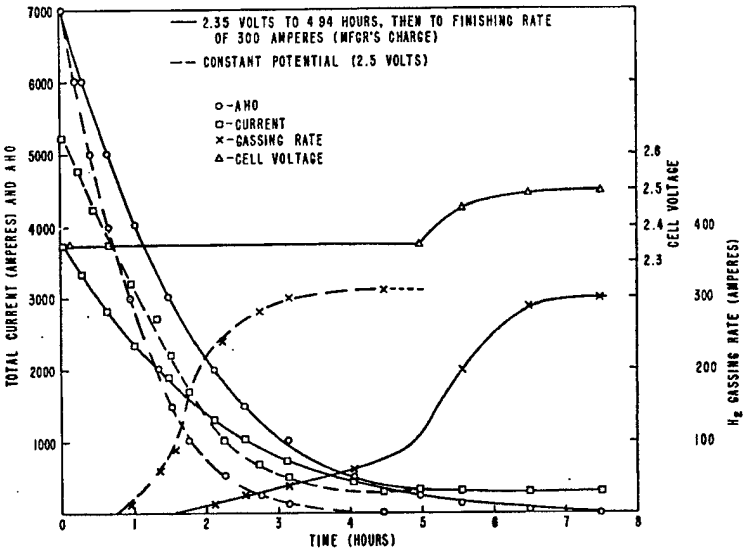

Figure 23 - Constructed constant-temperature (90°F) charges for MAQ cell after 7,000 AHO

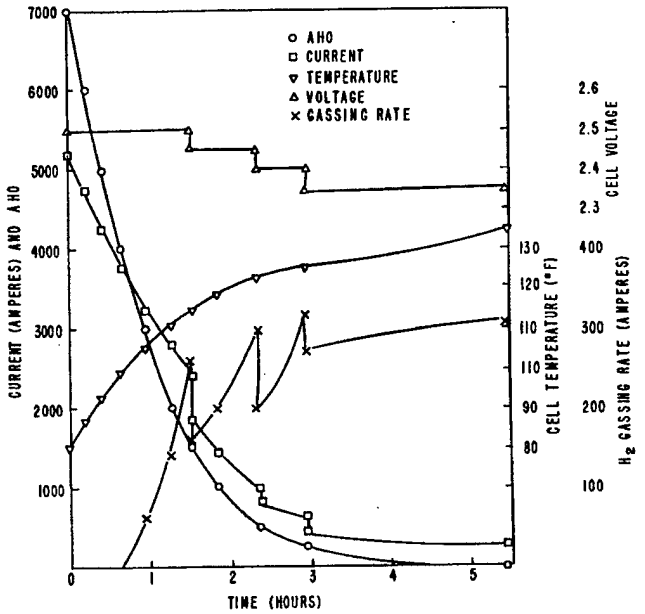

Figure 24 - Charge by experimental TVG curve with no cooling, initial cell temperature 80°F, MAQ cell

The role of temperature in limiting charging rates should be emphasized and explained for each of the limiting conditions. Where cell cooling is so efficient that constant temperatures can be maintained, the charge procedure is simplicity itself because only one charge voltage is established for maximum safe gassing at the end of charge, and it is such that charge will be put in in nearly minimum times. As an example, for a fully discharged MAQ cell, the charge voltage would be set at 2.4 volts (at 90° F) and full charge would be accomplished in about 4 hours. Slightly faster charges could be put in by starting at higher voltages and cutting back as gassing approaches the maximum safe value. It is not important that the amount of previous discharge be known; the charge is merely started at 2.5 volts and continued until the current value and the gassing rate, determined from the hydrogen and air flow-rate meters, become identical. Then the charge could be secured or allowed to gas for a while. As the effects of age come on, they will be shown by a gradually increasing finishing rate and longer charge times. The charge voltage would be decreased accordingly.

In the absence of cooling, because temperature is increasing during the course of the charge, the proper procedure to obtain minimum charge times is by no means so obvious. It may be stated quite definitely, however, that the minimum charge time is controlled by the initial cell temperature and the maximum cell temperature allowable at the end of charge. By preconstructing charge curves, it became evident, on a trial and error basis, that many different charge procedures could result in minimum charge times. For example, by sacrificing initial high rates for the sake of keeping temperature down, time can be made up at the end of charge. On the other hand, time is saved initially by the use of high-charge rates at the beginning; but the temperature goes up rapidly, and the last stages of charge are slowed down. There is, however, one charge procedure that will satisfy the requirements of minimum time and simplicity. This consists in charging the cell at a constant voltage for 90-95% of the $PbSO_4$ conversion. The voltage is determined by the initial cell temperature; the cell reaches maximum temperature and the maximum gassing limit just at the end of charge, after the voltage has been adjusted to 2.4 toward the end of charge. Of course, as the battery approaches the end of its useful life, the aging effect should come into play strongly; higher gassing rates will result in more heating, and the charge voltage will have to be decreased. The charge-voltage initial-temperature relationship has been worked out for the new MAQ cell under the following conditions: fully discharged, not cooled, and limited by a maximum gassing rate of 310 amperes and a maximum end-of-charge temperature of 120° F. Typical charges corresponding to different starting temperatures are shown in Figure 25. In Figure 26 the initial voltages of these charges are plotted against the initial temperature. The time for charge is also plotted against initial temperature; and on the same graph the time for constant-temperature charges, corresponding to the initial cell temperatures, is plotted for comparison.

Generally, in service today, only a comparatively inefficient cooling system is available, and so the time curves for charge would be expected to lie between curves 1 and 2 of Figure 26; their positions depend largely on the degree of efficiency of the cooling system. In the event of inefficient cooling, the voltage curve will also be raised somewhat. It is suggested that charging procedures in submarines, where only inefficient cooling is available, might be governed by a voltage curve such as that shown in Figure 26, and charges might be run as shown in Figure 25. This would replace the TVG curve. Such a procedure would be quite simple because it contains essentially only two steps, not counting the overcharge period, and does not sacrifice charging speed. The comparison between the two time curves of Figure 26 indicates the tactical and operational advantages which could result from efficient cooling.

It should be emphasized that in the absence of efficient cooling the high experimental TVG curve of Figure 19 is useless as a guide to charging procedure because initial high temperatures and prolonged charge times would result.

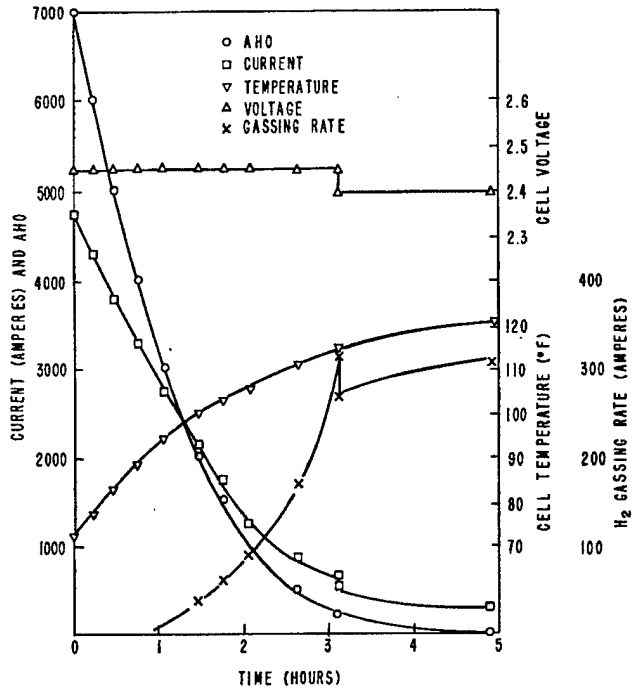

(a) 72° F

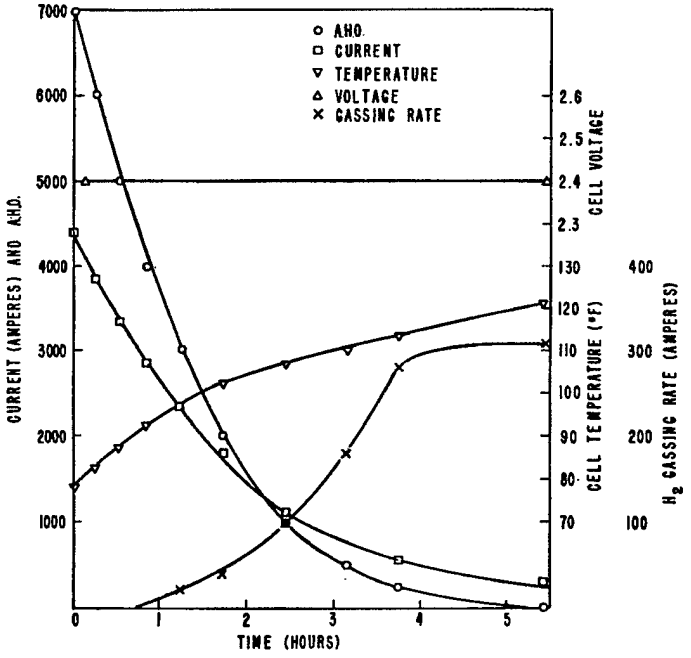

(b) 78° F

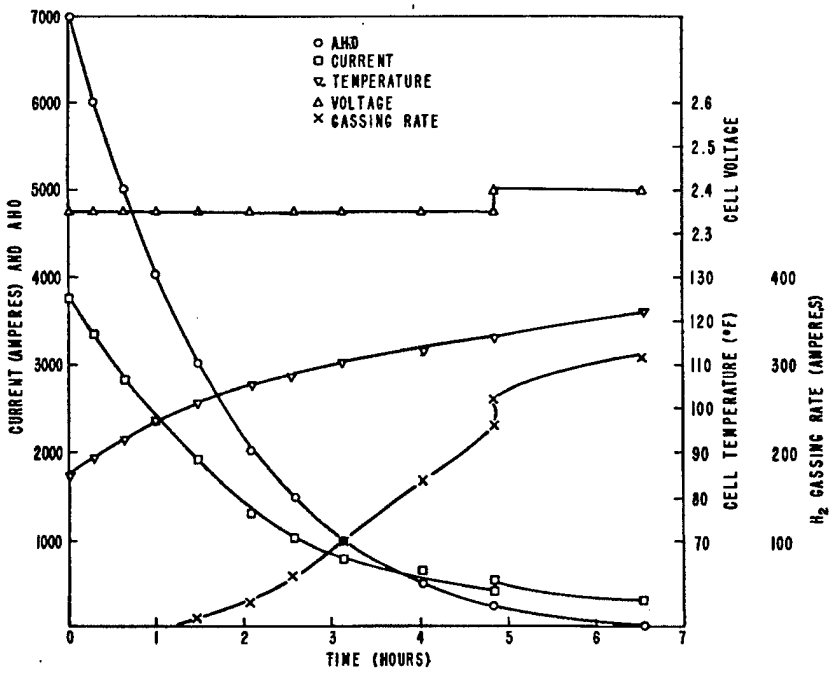

(c) 85° F

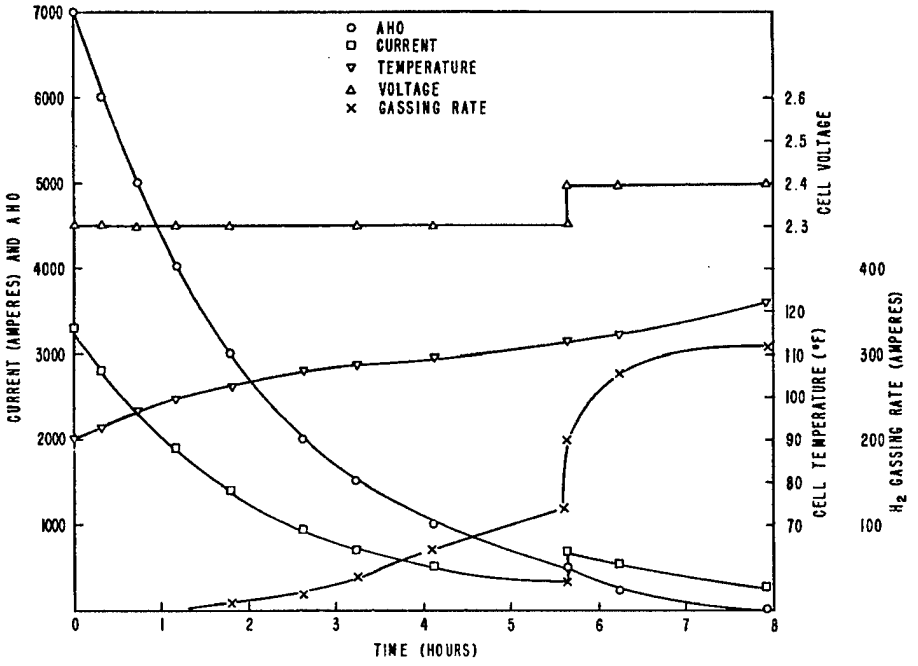

(d) 90° F

Figure 25 - Charge from various starting temperatures with no cooling, MAQ cell

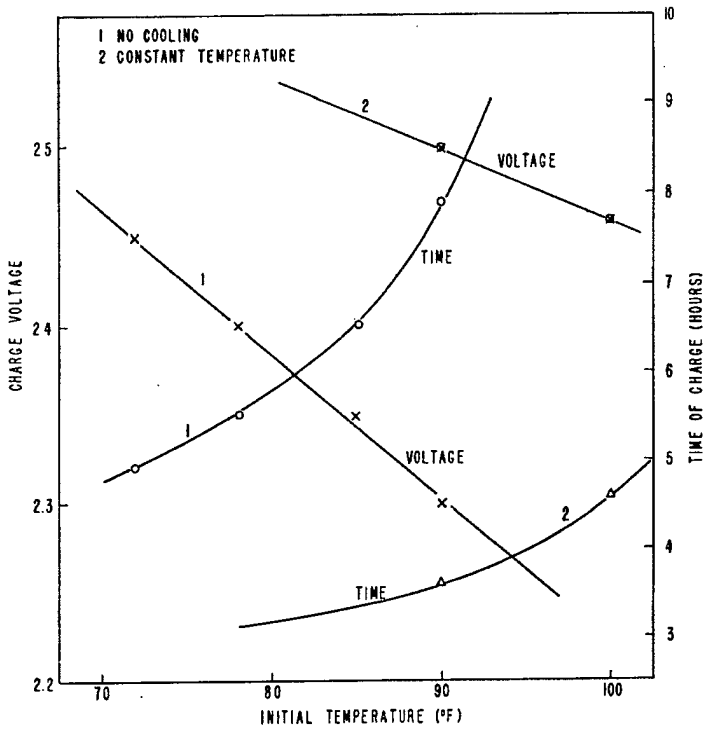

Figure 26 - Comparison of charge times and voltages for efficient cooling and no cooling, 7,000 AHO, MAQ cell

Here, again, the amount of previous discharge is of no particular concern because, if it is less than complete, charging times and temperatures will be lower than those shown by Figure 25. Indeed, for constant-potential charges, the value of current is a fair indication of the state of discharge, while the current minus the hydrogen gassing current is a good indication. The state of charge could be obtained with good approximation from a family of curves such as those of Figure 21. For example, if the total current during the course of charge at 2.35 volts were observed to be 1300 amperes and the hydrogen gassing current were about 70, the difference would be 1230, and reference to Figure 21 would show that $PbSO_4$ equivalent to about 1800-1900 ampere hours remained to be converted. Therefore, these curves might be of practical value in ordinary operation.

CELL DESIGN VS. GASSING AND CHARGE ACCEPTANCE

Another qualitative analysis will be attempted to show how some factors of cell design may be expected to influence gassing and charge acceptance. Concerning gassing, it is obvious that if a certain current density will establish a certain hydrogen overvoltage at a metal plate of a given area, the same current density will be necessary to give the same voltage at a plate with twice the area, but the total current flowing will be doubled. So it may be said that if two negative plates of different weights present equal area per unit weight to the solution, the heavier plate will require more current to give the same potential. This relationship among current, area, and potential will be given quantitatively by: $b \log I/A \propto V$, where I = gross current, A = area, V = cell voltage, and b = the slope of the overvoltage curve, or $\Delta V/\Delta \log I$. With this relation, the displacement in the TVG curve as a function of plate area may be estimated. Strictly speaking, the relation should not be applied to the whole cell voltage because it has been empirically established for single electrodes. b and V, however, should both increase proportionately as the effect of the

positive plate voltage is lumped in, and the relation will be used to give a qualitative estimation of the area effect. Such important factors as expanders, grid composition, proportion of grid weight to active material weight, and extent of poisoning will have unknown but large effects; so errors resulting from the application of the principle to a whole cell probably will not be important.

Consider first the relative displacement of the TVG curves for the OWTX and the VLA cells. The OWTX presents a gross negative plate area of 25,000 sq in. to the solution, while the VLA has an area of 22,200 sq in.; therefore it might be expected that the VLA will have a higher TVG curve than the OWTX, which it does. Using the previous relation, at the same current and temperature, the relative value of the voltages will be given by: $b \log A/A' = \Delta V$, where b may be assigned the value 0.4 for purposes of calculation. Substituting the above area values for A and A′ and 0.4 for b, ΔV is found to be 0.02 volt. Therefore, the OWTX should have a TVG curve about 0.02 volt lower than that for the VLA. Reference to Figure 7 shows that the actual difference is about 0.09. Differences in grid composition, degree of poisoning, and variation in the value of b between the two cells could easily account for the difference. Moreover, the OWTX has a thinner negative plate and probably presents more area per unit weight to the solution; so the calculated value should be larger on that account. Because of the lack of any definite knowledge as to how this correction should be applied and for the sake of an example, we may arbitrarily assume the effect to be linear with plate thickness; then the value 25,000 x 0.18/0.165 for the effective relative area of the OWTX would lead to a ΔV of 0.035 volt.

A comparison between the VLA and the MAQ may be made in similar fashion. Although the MAQ has less weight of active material than the VLA, it has more and thinner plates and has a gross negative plate area of 25,000 sq in. Using this figure, the TVG curve displacement would be calculated to be 0.02 volt. If a plate thickness correction is made, as above, the value becomes 0.14 volt. A comparison of Figures 19 and 7 shows the measured difference to be about 0.065.

Similar comparisons could be made between other types of submarine cells, but in the absence of any detailed knowledge of the complicating factors mentioned the procedure really amounts to no more than an exercise to illustrate the area effect.

Regarding the charge acceptance, it may be said that, where more plate area per unit weight of active material is exposed to the electrolyte, the slope of the CA vs. voltage curve will be higher; and as a result faster charging at similar voltages will be expected. All other things being equal, less heating will occur because charge time is faster. This conclusion was derived by comparing the charge acceptance of the OWTX and the VLA with that for the MAQ cell.

SUMMARY AND CONCLUSIONS

Charge data was obtained for OWTX and VLA submarine cells under a variety of conditions of temperature and voltage. From the gassing data, experimental TVG curves were constructed which are higher than the present TVG curve and show that higher charging voltages than those now used could be safe. The data was also used to show that the rate of conversion of $PbSO_4$ (charge acceptance) during charge is a linear function of voltage for the experimental cells and that it is nearly temperature insensitive over the ordinary operating range.

The charge-acceptance data in connection with the gassing data show that, if very efficient cooling is available, charging times can be made much faster, with safety, than those allowed by the present TVG curve. This would be expected to result in tactical and operational advantages to the submarine. The data show the minimum time for complete charge

to be limited by cell temperature, cell design–as it affects gassing and charge acceptance, and the maximum safe gassing rate. For a given cell design and an established safe gassing rate, temperature only will be the limiting factor.

Equations which are based on theory enable calculation of the heating effects within the cell; so that, in the absence of efficient cooling, the temperature rise of the cell during charge can be estimated sufficiently accurately.

Knowledge of gassing rates, charge acceptance, and heating and cooling effects enable the construction of charging curves for any conceivable type of charge; this in turn, allows the study and evaluation of charging procedures without a large amount of experimental work. Charging curves were constructed for the OWTX which show that under conditions of no cooling, charging time will be prolonged by starting at high rates and cutting back according to the TVG curve.

It is shown that gassing curves and charge-acceptance curves can be obtained from a small number of experimental charges so that charging curves can be constructed for study to determine best charging procedures. This means that charging procedures can be established for cells of new design without delay. The process was applied to a new MAQ cell, for which six sets of charge data were available.

In the absence of efficient cooling, for a given cell design and maximum gassing rate, minimum charge times are strictly dependent on the cell temperature at the start of charge and the maximum allowable temperature at the end of charge. Minimum charge times under these conditions may be met by a variety of charge procedures, but they may be accomplished quite simply by charging for 90-95% of active material conversion at a constant potential, which is defined by the initial cell temperature, and finishing the charge at some voltage which can be readily determined.

The effect of age on the TVG curve is shown by the experimental results, and its effect on charging procedures is considered qualitatively.

It is shown how charge acceptance may be used to estimate the state of discharge of a cell.

The effect of negative plate area on the position of the TVG curve can be estimated by comparison of cells, but complicating factors exist which render the procedure of qualitative significance only. Cell design is briefly considered in connection with charge acceptance.

* * *

REFERENCES

1. N. Y. Navy Yard,(Material Laboratory) "Report of Test on Charging Method and Temperature and Charging Effect on Tudor Type 20-POR-820 Submarine Storage Cells, etc.," Test No. 2527-A, July 2, 1934

2. Abbott, R. W.,and Lunn, E. G., "Studies of Methods of Determining the State of Charge of, and of Charging, Submarine Storage Batteries," Naval Research Laboratory, Dec. 30, 1932

3. Crockford, H. D.,and Sink, W. G., "Heat Balance Studies on Submarine Storage Cells – The Gassing Voltage – Gravity – Temperature Relationships in Lead-Acid Cells," NRL Report P-1195, Dec. 17, 1935

4. BuShips Letter S62-4 (660S-335),Feb. 12, 1945

5. Lander, J. J., "The Investigation of the Suitability of the Open-Cell Type of Battery Ventilation for Use Aboard Submarines," NRL Report 2675, Aug. 1945

* * *

NAVY-DPPO PRNC. WASH., D.C.

UNCLASSIFIED

ATI 186 785

Office of Naval Research, Naval Research Lab.,
Washington, D.C. (NRL Report 4075)

CHARGING PROCEDURES FOR SUBMARINE STORAGE BATTERIES, by E. E. Nelson, Isabelle M. Paige, and J. J. Lander. 7 Nov '52, 32 pp. incl. graphs.

Electrical Equipment (16)
Batteries and Storage (8)

Batteries - Charging
Submarines

(Copies obtainable from ASTIA-DSC.)

UNCLASSIFIED